

# Hybrid State Space and Frequency Domain System Level Synthesis for Sparsity-Promoting $\mathcal{H}_2/\mathcal{H}_\infty$ Control Design

Zhong Fang and Michael W. Fisher

**Abstract**—Design of optimal linear feedback controllers is a challenging but important problem in many applications. The main difficulties arise from nonconvexity and infinite dimensionality of the associated optimization problem for the design. A promising recent approach to address these challenges is to first use system level synthesis to render the problem convex using a clever reparameterization, and then to apply an approximation by simple poles to obtain a finite dimensional problem. However, when computing  $\mathcal{H}_2$  and  $\mathcal{H}_\infty$  norms, this prior approach requires an additional approximation of a finite time horizon for the closed-loop impulse response. This finite horizon results in increased suboptimality, degraded performance, and increased problem size and memory requirements. To address these limitations, we present a novel control design framework that combines the frequency domain system level synthesis constraints with a state space formulation of the  $\mathcal{H}_2$  and  $\mathcal{H}_\infty$  norms using linear matrix inequalities. This state space formulation eliminates the need for a finite time horizon approximation, and results in a convex and tractable semidefinite program for the control design. To preserve robustness, in practice it is important that controllers only contain a relatively small number of poles. Therefore, we propose to make an optimal sparse selection of simple poles from a large initial collection to maintain robustness while improving performance. As this sparsity constraint is nonconvex, we use group lasso regularization to enforce sparsity while maintaining convexity for the control design. Finally, the superior performance of the proposed method is illustrated on an example of power converter control design.

## I. INTRODUCTION

Optimal linear feedback control design is a challenging but valuable problem. The first major difficulty is that the design problem is nonconvex in the controller. Convex reparameterization, which involves a change of variables to render the optimization problem convex, is one approach to address this. A classical example is the Youla parametrization [1], while more recent methods include system level synthesis (SLS) [2] and the input output parametrization (IOP) [3]. The SLS and IOP methods have several advantages over Youla parameterization [4], including directly parameterizing the control design via the closed-loop system responses. For this work we are interested in state feedback design, whereas IOP is primarily intended for output feedback, and therefore focus on SLS.

Convex reparameterization methods result in convex control design problems, yet remain infinite dimensional and, hence, intractable in general. Different finite dimensional approximation methods have been proposed with SLS to

tackle this. In [5], the finite impulse response (FIR) approximation is used for the closed-loop system responses. This requires all closed-loop poles to lie at the origin, causing infeasibility for stabilizable but uncontrollable systems, high computational cost in systems with large separation of time scales, inability to incorporate prior knowledge about optimal closed-loop poles, and results in deadbeat control, which often has poor robustness to uncertainty and disturbances due to large control gains. The simple pole approximation (SPA) [6] was developed to circumvent these drawbacks by using poles of multiplicity one (i.e., simple poles) to approximate the closed-loop system responses. SPA gives the designer the freedom to form an approximation using any finite selection of stable poles in the unit disk that are closed under complex conjugation, and can therefore easily include prior knowledge about optimal closed-loop poles.

In prior work [7], SLS and SPA were combined in an attempt to solve the mixed  $\mathcal{H}_2/\mathcal{H}_\infty$  control design problem. However, to compute the  $\mathcal{H}_2$  and  $\mathcal{H}_\infty$  norms of the closed-loop system responses, [7] uses finite time horizon approximations of the closed-loop impulse response and convolution operators. This results in increased suboptimality leading to degraded performance, higher memory and storage requirements, and longer runtimes. Furthermore, in [7] a heuristic is used for the selection of the simple poles, without any attempt to choose them optimally, which results in increased suboptimality as well.

A hybrid state space and frequency domain formulation of the mixed  $\mathcal{H}_2/\mathcal{H}_\infty$  optimal control design is proposed to address the limitations of SLS with SPA. SLS requires additional constraints, which are affine if expressed in the frequency domain. Therefore, our method maintains this frequency domain representation of the SLS constraints. However, unlike in prior work [7], we use the Kalman-Yakubovich-Popov (KYP) lemma to express the  $\mathcal{H}_2$  and  $\mathcal{H}_\infty$  norms of the closed-loop system responses in state space in the form of linear matrix inequalities (LMIs). To do so, we use the simple pole approximation to obtain state space realizations of the closed-loop system responses. Our method does not require any finite time horizon approximation, and thus does not suffer from the drawbacks discussed above. The resulting control design problem is a convex and tractable semidefinite program which can be solved accurately and efficiently.

The heuristic selection of simple poles in [7] requires a large number of poles to reduce the suboptimality of the approximation. However, this increases the computational cost of the design problem, and reduces the robustness

Z. Fang and M. W. Fisher are with the Department of Electrical and Computer Engineering, University of Waterloo, Waterloo, Ontario, Canada (e-mail: {z4fang, michael.fisher}@uwaterloo.ca).

of the resulting controller. Therefore, we propose to start with a large collection of potential poles, and choose the sparse selection from them that results in optimal fixed-order performance. As this sparsity constraint is nonconvex, we adopt the group lasso method [8], an extension of the lasso method (i.e.,  $l_1$  regularization) to selection of grouped factors, to enforce sparsity while maintaining convexity. This preserves tractability of the control design method, while reducing suboptimality of the closed-loop pole selection. An example of power converter control design demonstrates superior performance of the method.

The rest of this paper is structured as follows. Section II introduces the problem formulation. Section III provides a valuable state space realization of the closed-loop system. The main results on the novel control design method are shown in Section IV. The derivation of the control design methods is presented in Section V. A numerical example is provided in Section VI. Finally, Section VII offers concluding remarks.

*Notation:* The superscript “ $\top$ ” and  $\text{Tr}\{\cdot\}$  denote the transpose and trace of a matrix, respectively. For a complex number  $z$ , let  $\text{Re}(z)$ ,  $\text{Im}(z)$ , and  $\bar{z}$  represent the real part, imaginary part, and complex conjugate of  $z$ . For any matrix  $A$ , its Frobenius norm is written as  $\|A\|_F = \sqrt{A^\top A}$ , and we define  $\delta(A) = 1$  if  $A$  is nonzero and  $\delta(A) = 0$  if  $A = 0$ . We say a matrix  $A$  is Schur if all of its eigenvalues have modulus less than one. A positive definite (semidefinite) matrix  $P$  is denoted by  $P \succ 0$  ( $P \succeq 0$ ). The set of real (symmetric) matrices of dimension  $n \times m$  ( $n \times n$ ) is denoted by  $\mathbb{R}^{n \times m}$  ( $\mathbb{S}^n$ ).  $0_n$  and  $I_n$  are the  $n \times n$  zero and identity matrices, and  $n$  is often omitted if there is no ambiguity. For any set  $S$ , let  $|S|$  be its cardinality (i.e., the number of elements it contains). Let  $\mathcal{M}$  denote a collection of matrices  $\{M_i\}_{i=1}^l$ , define the block diagonal concatenation operator by  $\mathcal{D}(\mathcal{M}) := \begin{bmatrix} M_1 & & \\ & \ddots & \\ & & M_\ell \end{bmatrix}$  where the off-diagonal entries are all zero, and define the block row concatenation operator by  $\mathcal{R}(\mathcal{M}) := [M_1 \ \cdots \ M_\ell]$ . The operator  $\otimes$  denotes the Kronecker product between any two matrices. We denote the set of real, rational, proper, and stable transfer function matrices as  $\mathcal{RH}_\infty$ , and the subset of  $\mathcal{RH}_\infty$  that are strictly proper as  $\frac{1}{z}\mathcal{RH}_\infty$ .

## II. PROBLEM STATEMENT AND BACKGROUND

Consider the linear time-invariant (LTI) system in discrete time described by the following state space representation:

$$\begin{aligned} x(k+1) &= Ax(k) + Bu(k) + \hat{B}w(k) \\ y(k) &= Cx(k) \end{aligned} \quad (1)$$

where  $x(k) \in \mathbb{R}^n$ ,  $u(k) \in \mathbb{R}^p$ ,  $w(k) \in \mathbb{R}^q$ ,  $y(k) \in \mathbb{R}^m$  are the state, controller signal, disturbance input, and performance output vectors at time step  $k$ , respectively. It will be useful to define the signal  $v(k) = \hat{B}w(k)$ .

Consider a linear state feedback control law of the form  $u(z) = K(z)x(z)$  where  $K$  is a dynamic controller. The closed-loop transfer function mapping disturbance  $w$  to output  $y$  is  $T_{w \rightarrow y}(z)$ , and  $T_{w \rightarrow u}(z)$ ,  $T_{v \rightarrow x}(z)$ , and  $T_{v \rightarrow u}(z)$  are

defined analogously. Let  $T_{\text{des}}(z)$  be some desired closed-loop transfer function for model matching control design, which can also be set to zero if preferred.

The goal of this paper is to design a controller  $K(z)$  that is a solution to the mixed  $\mathcal{H}_2/\mathcal{H}_\infty$  control design problem given by

$$\begin{aligned} \min_{K(z)} & \left\| \begin{bmatrix} Q & 0 \\ 0 & R \end{bmatrix} \begin{bmatrix} T_{w \rightarrow y}(z) - T_{\text{des}}(z) \\ T_{w \rightarrow u}(z) \end{bmatrix} \right\|_{\mathcal{H}_2/\mathcal{H}_\infty} \\ \text{s.t.} & \quad T_{v \rightarrow x}(z), T_{v \rightarrow u}(z) \in \frac{1}{z}\mathcal{RH}_\infty \end{aligned} \quad (2)$$

where the mixed  $\mathcal{H}_2/\mathcal{H}_\infty$  norm is given by  $\|T\|_{\mathcal{H}_2/\mathcal{H}_\infty} = \|T\|_{\mathcal{H}_2} + \lambda\|T\|_{\mathcal{H}_\infty}$  for some constant  $\lambda \in [0, \infty]$ . The constant matrices  $Q$  and  $R$  represent the weights on output and input, respectively. Note that (2) is nonconvex in  $K(z)$  since  $T_{w \rightarrow y}(z)$  and  $T_{w \rightarrow u}(z)$  are, so this problem is challenging to solve in this form.

Using SLS, (2) can be equivalently reformulated as follows (we refer the reader to [2] for further details about SLS)

$$\min_{\Phi_x(z), \Phi_u(z)} \left\| \begin{bmatrix} Q & 0 \\ 0 & R \end{bmatrix} \begin{bmatrix} \tilde{\Phi}_x(z) - T_{\text{des}}(z) \\ \tilde{\Phi}_u(z) \end{bmatrix} \right\|_{\mathcal{H}_2/\mathcal{H}_\infty} \quad (3a)$$

$$\text{s.t.} \quad (zI - A)\Phi_x(z) - B\Phi_u(z) = I \quad (3b)$$

$$\Phi_x(z), \Phi_u(z) \in \frac{1}{z}\mathcal{RH}_\infty \quad (3c)$$

where  $\Phi_x(z)$  and  $\Phi_u(z)$  are the design variables and represent the closed-loop transfer functions  $T_{v \rightarrow x}(z)$  and  $T_{v \rightarrow u}(z)$ , respectively, and where  $\tilde{\Phi}_x(z) = T_{w \rightarrow y}(z) = C\Phi_x(z)\hat{B}$  and  $\tilde{\Phi}_u(z) = T_{w \rightarrow u}(z) = \Phi_u(z)\hat{B}$ . Note that (3c) ensures stability and well-posedness of the closed-loop system. SLS requires the additional affine constraint (3b). Note that (3) is now convex, although still infinite dimensional as  $\Phi_x(z)$  and  $\Phi_u(z)$  lie in the infinite dimensional function space  $\frac{1}{z}\mathcal{RH}_\infty$ .

To circumvent this issue, [7] approximates the closed-loop transfer functions using a finite selection of simple stable poles  $\mathcal{P}$ , closed under complex conjugation, as

$$\Phi_x(z) = \sum_{p \in \mathcal{P}} G_p \frac{1}{z - p}, \quad \Phi_u(z) = \sum_{p \in \mathcal{P}} H_p \frac{1}{z - p}, \quad (4)$$

where  $G_p$  and  $H_p$  are (complex) coefficient matrices for each  $p \in \mathcal{P}$ . This simple pole approximation (SPA) renders (3) finite dimensional. In [6] it is proposed to select the closed-loop poles  $\mathcal{P}$  along an Archimedes spiral in the unit disk. It was then shown in [7, Corollary 1] that for this pole selection, the solution to (3) with the SPA (4) satisfies the following suboptimality bound

$$\frac{J(\mathcal{P}_n) - J^*}{J^*} \leq \frac{\hat{K}}{\sqrt{n}}, \quad (5)$$

where  $\hat{K}$  is a constant that depends on the ground-truth optimal solution,  $J^*$  is the ground-truth optimal cost of problem (3), and  $J(\mathcal{P}_n)$  is the optimal cost of (3) with the SPA (4) for the selection  $\mathcal{P}_n$  of  $n$  poles from the Archimedes spiral. By (5), the suboptimality of the solution of SLS with SPA will tend to zero as the number of poles approaches

infinity. However, (5) was derived under the assumption that (3) with (4) could be solved exactly, but this was not the case in [7] due to a finite time horizon approximation used to calculate the  $\mathcal{H}_2$  and  $\mathcal{H}_\infty$  norms, so the suboptimality may not tend to zero as the number of poles diverges for the method in [7].

For SPA, since  $\Phi_x(z)$  and  $\Phi_u(z)$  are real, it is straightforward to show that for any real pole  $p$ ,  $G_p$  and  $H_p$  are real, and for any complex pole  $p$ ,  $G_{\bar{p}} = \overline{G_p}$  and  $H_{\bar{p}} = \overline{H_p}$ . Let  $\mathcal{P}_r$  denote the real poles in  $\mathcal{P}$ , and let  $\mathcal{P}_c$  denote its complex poles. Then  $\mathcal{P} = \mathcal{P}_r \cup \mathcal{P}_c$ .

### III. CLOSED-LOOP REALIZATION

To derive the proposed hybrid state space and frequency domain control design method, we will require state space realizations of the closed-loop transfer functions. In this section, we propose novel state space realizations of the closed-loop dynamics based on the simple pole approximation.

For any  $p \in \mathcal{P}_c$ , its conjugate  $\bar{p}$  is also in  $\mathcal{P}_c$ , their corresponding coefficient matrices are:

$$\begin{aligned} G_p &= \text{Re}(G_p) + \text{Im}(G_p)j, & G_{\bar{p}} &= \text{Re}(G_p) - \text{Im}(G_p)j, \\ H_p &= \text{Re}(H_p) + \text{Im}(H_p)j, & H_{\bar{p}} &= \text{Re}(H_p) - \text{Im}(H_p)j. \end{aligned} \quad (6)$$

We first find real state space realizations for  $\tilde{\Phi}_x(z)$  and  $\tilde{\Phi}_u(z)$ . To do so, for each complex conjugate pair  $p, \bar{p} \in \mathcal{P}_c$ , define the matrix

$$M(p) = \begin{bmatrix} \text{Re}(p) & \text{Im}(p) \\ -\text{Im}(p) & \text{Re}(p) \end{bmatrix},$$

and let  $\mathcal{M}_c$  be the collection of  $M(p)$  for all such complex conjugate pairs. Let  $\mathcal{M}_r$  be the collection of each scalar matrix  $p$  for all  $p \in \mathcal{P}_r$ . Then we can define

$$\begin{aligned} \bar{A} &= \begin{bmatrix} \mathcal{D}(\mathcal{M}_r) & \\ & \mathcal{D}(\mathcal{M}_c) \end{bmatrix} \otimes I, \\ \bar{B} &= \begin{bmatrix} I & \cdots & I & 2I & 0 & \cdots & 2I & 0 \end{bmatrix}^\top \hat{B}. \end{aligned}$$

$\underbrace{\hspace{1.5cm}}_{|\mathcal{P}_r|} \quad \underbrace{\hspace{1.5cm}}_{|\mathcal{P}_c|}$

Next, for each complex conjugate pair  $p, \bar{p} \in \mathcal{P}_c$ , define the matrices

$$G(p) = [\text{Re}(G_p) \quad \text{Im}(G_p)], \quad H(p) = [\text{Re}(H_p) \quad \text{Im}(H_p)],$$

and let  $\mathcal{G}_c$  and  $\mathcal{H}_c$  be the collection of  $G(p)$  and  $H(p)$ , respectively, for all such complex conjugate pairs. Let  $\mathcal{G}_r$  and  $\mathcal{H}_r$  be the collection of  $G_p$  and  $H_p$ , respectively, for each  $p \in \mathcal{P}_r$ . Then we define

$$\begin{aligned} \bar{C}_x &= C [\mathcal{R}(\mathcal{G}_r) \quad \mathcal{R}(\mathcal{G}_c)], \\ \bar{C}_u &= [\mathcal{R}(\mathcal{H}_r) \quad \mathcal{R}(\mathcal{H}_c)]. \end{aligned}$$

It is straightforward to verify that  $(\bar{A}, \bar{B}, \bar{C}_x, 0)$  is a real state space realization of  $\tilde{\Phi}_x(z)$ , and that  $(\bar{A}, \bar{B}, \bar{C}_u, 0)$  is a real state space realization of  $\tilde{\Phi}_u(z)$ . To see this, first note that  $\tilde{\Phi}_x(z)$  and  $\tilde{\Phi}_u(z)$  can be decomposed into the contributions from individual real poles and from complex

conjugate pairs of poles since  $\bar{A}$  is block diagonal. For any real pole  $p$ , it follows

$$CG_p [zI - pI]^{-1} \hat{B} = CG_p \frac{1}{z - p} \hat{B}.$$

For any complex conjugate pair of poles  $p$  and  $\bar{p}$ ,

$$\begin{aligned} & [\text{Re}(G_p) \quad \text{Im}(G_p)] \begin{bmatrix} zI - \text{Re}(p)I & -\text{Im}(p)I \\ \text{Im}(p)I & zI - \text{Re}(p)I \end{bmatrix}^{-1} \begin{bmatrix} 2I \\ 0 \end{bmatrix} \\ &= [\text{Re}(G_p) \quad \text{Im}(G_p)] \frac{1}{(z - p)(z - \bar{p})} \begin{bmatrix} 2zI - 2\text{Re}(p)I \\ -2\text{Im}(p)I \end{bmatrix} \\ &= \frac{2z\text{Re}(G_p) - 2\text{Re}(G_p)\text{Re}(p) - 2\text{Im}(G_p)\text{Im}(p)}{(z - p)(z - \bar{p})} \\ &\stackrel{(6)}{=} G_p \frac{1}{z - p} + G_{\bar{p}} \frac{1}{z - \bar{p}} \end{aligned} \quad (7)$$

and  $C \left( G_p \frac{1}{z - p} + G_{\bar{p}} \frac{1}{z - \bar{p}} \right) \hat{B}$  can be obtained by left multiplying (7) by  $C$  and right multiplying (7) by  $\hat{B}$ . Therefore  $(\bar{A}, \bar{B}, \bar{C}_x, 0)$  is a real state space realization of  $\tilde{\Phi}_x(z)$ , and  $(\bar{A}, \bar{B}, \bar{C}_u, 0)$  can be shown to be a real state space realization of  $\tilde{\Phi}_u(z)$  analogously.

Let  $(A_{\text{des}}, B_{\text{des}}, C_{\text{des}}, 0)$  be any real state space realization of  $T_{\text{des}}$ . Now we can represent the transfer function in the objective (3a) using the following real state space realization

$$\tilde{A} = \begin{bmatrix} \bar{A} & 0 \\ 0 & A_{\text{des}} \end{bmatrix}, \quad \tilde{B} = \begin{bmatrix} \bar{B} \\ B_{\text{des}} \end{bmatrix}, \quad \tilde{C} = \begin{bmatrix} Q\bar{C}_x & -QC_{\text{des}} \\ R\bar{C}_u & 0 \end{bmatrix}, \quad (8)$$

which satisfies

$$\tilde{C}(zI - \tilde{A})^{-1} \tilde{B} = \begin{bmatrix} Q & 0 \\ 0 & R \end{bmatrix} \begin{bmatrix} \tilde{\Phi}_x(z) - T_{\text{des}}(z) \\ \tilde{\Phi}_u(z) \end{bmatrix} =: \Phi(z). \quad (9)$$

Thus, we have obtained an equivalent state space representation of the closed-loop transfer function  $\Phi(z)$ , which will be used to develop our novel control design method. Note that for a fixed collection of simple poles  $\mathcal{P}$ , as used for SPA,  $\bar{A}$  and  $\bar{B}$  are constant matrices, and  $\tilde{C}$  is an affine function of all of the variable coefficients  $G_p$  and  $H_p$ .

### IV. MAIN RESULTS

#### A. Hybrid State Space and Frequency Domain Design

In this section we present our hybrid state space and frequency domain control design method which does not require any finite time horizon approximations for computing the  $\mathcal{H}_2$  and  $\mathcal{H}_\infty$  norms of the closed-loop transfer functions. As a result, it has reduced suboptimality, better performance, and lower computational cost compared to prior work [7]. The full derivation of the method is presented in Section V, but the key idea is to use the state space realizations provided in Section III together with the KYP lemma to derive an equivalent state space representation of the  $\mathcal{H}_2$  and  $\mathcal{H}_\infty$  norms of the closed-loop transfer functions as LMIs. However, the additional SLS constraints required for the SLS formulation no longer remain affine if we represent them in state space, so we choose to retain their frequency domain representation. Combining these two representations,

we obtain the following control design formulation for the solution to (3) with the SPA (4)

$$\min_{K_1, K_2, Z, G_p, H_p, \gamma_1, \gamma_2} \gamma_1 + \lambda \gamma_2 \quad (10a)$$

$$\text{s.t.} \quad \begin{bmatrix} K_1 & K_1 \tilde{A} & K_1 \tilde{B} \\ \tilde{A}^\top K_1 & K_1 & 0 \\ \tilde{B}^\top K_1 & 0 & \gamma_1 I \end{bmatrix} \succ 0 \quad (10b)$$

$$\begin{bmatrix} K_1 & 0 & \tilde{C}(G_p, H_p)^\top \\ 0 & I & 0 \\ \tilde{C}(G_p, H_p) & 0 & Z \end{bmatrix} \succ 0 \quad (10c)$$

$$\text{Tr}(Z) < \gamma_1 \quad (10d)$$

$$\begin{bmatrix} K_2 & 0 & \tilde{A}^\top K_2 & \tilde{C}(G_p, H_p)^\top \\ 0 & \gamma_2 I & \tilde{B}^\top K_2 & 0 \\ K_2 \tilde{A} & K_2 \tilde{B} & K_2 & 0 \\ \tilde{C}(G_p, H_p) & 0 & 0 & \gamma_2 I \end{bmatrix} \succ 0 \quad (10e)$$

$$\sum_{p \in \mathcal{P}_r} G_p + 2 \sum_{p \in \mathcal{P}_c} \text{Re}(G_p) = I \quad (10f)$$

$$(pI - A)G_p - BH_p = 0, \quad p \in \mathcal{P}_r \quad (10g)$$

$$(\text{Re}(p)I - A)\text{Re}(G_p) - \text{Im}(p)\text{Im}(G_p) - B\text{Re}(H_p) = 0, \quad p \in \mathcal{P}_c \quad (10h)$$

$$(\text{Re}(p)I - A)\text{Im}(G_p) + \text{Im}(p)\text{Re}(G_p) - B\text{Im}(H_p) = 0, \quad p \in \mathcal{P}_c \quad (10i)$$

where  $K_1, K_2 \in \mathbb{S}^{n \times |P|}$ ,  $Z \in \mathbb{S}^m$ , and  $\gamma_1, \gamma_2$  are scalar variables that represent the  $\mathcal{H}_2$  and  $\mathcal{H}_\infty$  norms of the closed-loop transfer functions, respectively. Recall that  $\tilde{A}$ ,  $\tilde{B}$ , and  $\tilde{C}$  were defined in (8), but we write  $\tilde{C} = \tilde{C}(G_p, H_p)$  to emphasize that  $\tilde{C}$  is an affine function of the coefficients  $G_p$  and  $H_p$  for all  $p \in \mathcal{P}$ . Since, using SPA, we have already selected the closed-loop poles  $\mathcal{P}$ ,  $\tilde{A}$  and  $\tilde{B}$  are constant matrices, along with  $A$ ,  $B$ , and  $C$ . Thus, the objective (10a) is linear, the constraints (10g)-(10i) are linear, the constraint (10f) is affine, and the constraints (10b)-(10e) are LMIs in the decision variables. Therefore, overall (10) is a convex semidefinite program (SDP) that can be solved efficiently. Note that the state space realizations of the closed-loop transfer functions from Section III were deliberately constructed to ensure that the constraints (10b)-(10e) become LMIs rather than nonconvex bilinear matrix inequalities by including all the decision variables  $G_p, H_p$  in  $\tilde{C}$  and leaving  $\tilde{A}, \tilde{B}$  as constant matrices.

As we will see in Section V, the objective (10a) and constraints (10b)-(10e) are derived from a state space representation, whereas the constraints (10f)-(10i) represent the SLS constraints in the frequency domain, which together yield a truly hybrid control design. Notably, the design method (10) exactly determines the  $\mathcal{H}_2$  and  $\mathcal{H}_\infty$  norms of the closed-loop transfer function, whereas [7] using Frobenius and spectral norms, respectively, to approximate them over a finite time horizon. The error of this finite time horizon approximation is thus entirely eliminated by the proposed design approach. As a result, for the Archimedes spiral pole selection proposed in [6], the suboptimality bound (5) from [7] applies exactly to (10), and ensures that the suboptimality

converges to zero as the number of poles approaches infinity. As we will see in the numerical example in Section VI, even a small number of poles can often result in low suboptimality, and thus good performance, in practice.

### B. Design with Sparsity-Promoting Pole Selection

As mentioned in Section IV-A, increasing the number of poles in the SPA pole selection will reduce the suboptimality, but it also reduces robustness of the resulting controller. Therefore, it is valuable to start with a large initial selection of poles, and then to use a sparsity constraint to optimally select a smaller number of final closed-loop poles. Towards that end, we introduce the sparsity constraint

$$\sum_{p \in \mathcal{P}} \delta(G_p) \leq l, \quad \sum_{p \in \mathcal{P}} \delta(H_p) \leq l \quad (11)$$

into the problem (10), where  $l$  is a positive integer, to limit the number of nonzero coefficient matrices  $G_p$  of  $\Phi_x$  and  $H_p$  of  $\Phi_u$ . Note that for any pole  $p \in \mathcal{P}$  such that  $G_p = 0$  and  $H_p = 0$ , that pole will not appear in the closed-loop transfer functions  $\Phi_x$  and  $\Phi_u$ , and therefore will not influence these closed-loop dynamics. Thus, (11) ensures that only a sparse selection of at most  $l$  closed-loop poles will be selected in the final control design. Choosing state space realizations for the final controller as in [2, Section 4], this will also impose a fixed-order constraint on the controller itself, and one can choose  $l$  to achieve any desired controller order.

Unfortunately, (11) is nonconvex, so to retain a tractable convex formulation for the control design while still enforcing sparsity, we instead use a convex regularization term in the objective. In particular, since the sparsity constraint in (11) involves coefficient matrices rather than scalars, group lasso, as an extension of lasso or  $l_1$ -norm regularization, is used to enforce sparsity of these matrices [8]. To do so, we take the Frobenius norm of the coefficient matrices, resulting in modifying the objective function (10a) to include a penalty term as follows

$$\gamma_1 + \lambda \gamma_2 + \sigma_x \sum_{p \in \mathcal{P}} \|G_p\|_F^2 + \sigma_u \sum_{p \in \mathcal{P}} \|H_p\|_F^2, \quad (12)$$

where  $\sigma_x, \sigma_u > 0$  are scalar weights that determine our emphasis on the sparsity of the pole selection according to the objective (3a). In particular, increasing  $\sigma_x$  and  $\sigma_u$  will typically result in a smaller pole selection. Combining this new objective function (12) with our previous constraints (10b)-(10i) results in a new optimization problem which allows us to make a sparse selection of poles from a large initial collection. Then, after making this optimal selection of closed-loop poles, we can use the control design method from Section IV-A for the final control design. As the constraints (10b)-(10i) are linear matrix inequalities and affine equalities, and since the objective function (12) is quadratic, this new optimization problem for the sparse pole selection is a convex conic program that can be solved efficiently. The example of Section VI demonstrates that the optimal sparse pole selection using the method from this section shows superior performance compared to the spiral pole selection of [6].

## V. CONTROL DESIGN DERIVATION

This section presents the derivation of our control design optimization problem (10). We begin with the problem formulation of SLS (3) together with SPA (4). First we will derive the representation of the SLS constraints (3b) for SPA, and then we will derive the state space representation of the objective function (3a).

For the SLS constraint (3b), substituting in the SPA (4) and matching coefficients of  $\frac{1}{z-p}$  for each pole  $p \in \mathcal{P}$  since these functions are linearly independent, we obtain

$$I = \sum_{p \in \mathcal{P}_r} G_p + 2 \sum_{p \in \mathcal{P}_c} \text{Re}(G_p) \quad (13)$$

for the constant term,

$$0 = (pI - A)G_p - BH_p \quad (14)$$

for each  $p \in \mathcal{P}_r$ , and

$$\begin{aligned} 0 &= (\text{Re}(p)I - A)\text{Re}(G_p) - \text{Im}(p)\text{Im}(G_p) - B\text{Re}(H_p) \\ 0 &= (\text{Re}(p)I - A)\text{Im}(G_p) + \text{Im}(p)\text{Re}(G_p) - B\text{Im}(H_p) \end{aligned} \quad (15)$$

for each complex conjugate pair  $p, \bar{p} \in \mathcal{P}_c$ . Thus, the SLS constraint (3b) with the SPA (4) can be equivalently represented using (13)-(15).

Next, we will express the  $\mathcal{H}_2$  and  $\mathcal{H}_\infty$  norms of the closed-loop transfer functions from the objective function (3a) using a state space representation. To do so, we begin with the real state space realization  $(\tilde{A}, \tilde{B}, \tilde{C}, 0)$  from (8), which is a realization of the closed-loop transfer function  $\Phi(z)$  by (9). In order to calculate the objective (3a), we need to express  $\|\Phi(z)\|_{\mathcal{H}_2}$  and  $\|\Phi(z)\|_{\mathcal{H}_\infty}$  in terms of LMIs using a state space representation. To accomplish this, we apply the KYP lemma to obtain bounds on the  $\mathcal{H}_2$  and  $\mathcal{H}_\infty$  norms of our state space representation  $(\tilde{A}, \tilde{B}, \tilde{C}, 0)$ . This yields the following result from [9, Section 4.6]

*Theorem 1:* For the transfer function  $\Phi(z) = \tilde{C}(zI - \tilde{A})^{-1}\tilde{B}$ , if  $\tilde{A}$  is Schur then the following statements hold.

(1)  $\|\Phi(z)\|_{\mathcal{H}_2} < \gamma_1$  if and only if there exist  $K_1 \in \mathbb{S}^{n \times |\mathcal{P}|}$ ,  $Z \in \mathbb{S}^m$ , such that

$$\begin{aligned} \begin{bmatrix} K_1 & K_1 \tilde{A} & K_1 \tilde{B} \\ \tilde{A}^\top K_1 & K_1 & 0 \\ \tilde{B}^\top K_1 & 0 & \gamma_1 I \end{bmatrix} &\succ 0, \\ \begin{bmatrix} K_1 & 0 & \tilde{C}^\top \\ 0 & I & 0 \\ \tilde{C} & 0 & Z \end{bmatrix} &\succ 0, \\ \text{Tr}(Z) &< \gamma_1. \end{aligned} \quad (16)$$

(2)  $\|\Phi(z)\|_{\mathcal{H}_\infty} < \gamma_2$  if and only if there exists  $K_2 \in \mathbb{S}^{n \times |\mathcal{P}|}$ ,

$$\begin{bmatrix} K_2 & 0 & \tilde{A}^\top K_2 & \tilde{C}^\top \\ 0 & \gamma_2 I & \tilde{B}^\top K_2 & 0 \\ K_2 \tilde{A} & K_2 \tilde{B} & K_2 & 0 \\ \tilde{C} & 0 & 0 & \gamma_2 I \end{bmatrix} \succ 0. \quad (17)$$

Note that  $\tilde{A}$  is Schur by construction because its eigenvalues consist of the poles  $\mathcal{P}$  from SPA, which all lie inside the unit disk, so the assumptions of Theorem 1 are

automatically satisfied. To use Theorem 1 to reexpress the objective function (3a), we note that

$$\min_{\Phi(z) \in \frac{1}{z} \mathcal{R} \mathcal{H}_\infty} \|\Phi(z)\|_{\mathcal{H}_2} + \lambda \|\Phi(z)\|_{\mathcal{H}_\infty}$$

is equivalent to

$$\min_{\gamma_1, \gamma_2, \Phi(z) \in \frac{1}{z} \mathcal{R} \mathcal{H}_\infty} \gamma_1 + \lambda \gamma_2 \quad (18a)$$

$$\text{s.t. } \|\Phi(z)\|_{\mathcal{H}_2} < \gamma_1 \quad (18b)$$

$$\|\Phi(z)\|_{\mathcal{H}_\infty} < \gamma_2 \quad (18c)$$

since the two inequalities  $\|\Phi(z)\|_{\mathcal{H}_2} < \gamma_1$  and  $\|\Phi(z)\|_{\mathcal{H}_\infty} < \gamma_2$  will become tight at optimality. Now we can apply Theorem 1 to (18) to express the objective function (3a) equivalently in terms of LMIs. Thus, combining (16), (17), (18a), and (13)-(15), we arrive at the final control design optimization problem (10), which is equivalent to (3) with the SPA (4).

## VI. NUMERICAL EXAMPLE

In this section, we demonstrate the proposed control synthesis method on the control of a wind turbine interfaced to the power grid via a power converter. We model the turbine and converter system using the model proposed in [10]. Let  $w$  represent the frequency and voltage magnitude at the connection point, and let  $y$  represent the power output of the converter. Then this can be formulated in the form of (1) with matrices given by

$$\begin{aligned} A &= \begin{bmatrix} 0.8046 & 0 & 0 & 0 \\ 0 & 0.1177 & -0.0112 & -0.1332 \\ 1 & 0 & 0 & 0 \\ 0 & 0 & 0 & 0.9889 \\ 0 & 0 & 0 & 0 \end{bmatrix}, B = \begin{bmatrix} 0 & 0 \\ 0 & 0 \\ 0.0111 & 0 \\ 0 & 1 \end{bmatrix}, \\ C &= \begin{bmatrix} 0 & 0.9066 & -0.0364 & 1.0218 & 0 \\ 0 & 0.364 & 0.9066 & -0.2406 & -1.0201 \end{bmatrix}, \hat{B} = \begin{bmatrix} -0.4885 & 0 \\ 0 & 1.0069 \\ 2.5 & 0 \\ 0 & 0 \\ 0 & 0 \end{bmatrix}, \\ A_{\text{des}} &= \begin{bmatrix} 0.944 & \\ & 0.944 \end{bmatrix}, B_{\text{des}} = \begin{bmatrix} -1.1052 & \\ & -1.1389 \end{bmatrix}, C_{\text{des}} = I_2. \end{aligned}$$

For the control design, we choose  $Q = I_2$ ,  $R = 0.01I_2$ , and  $\lambda = 0.5$ . For the sparsity-promoting optimization, we choose  $\sigma_x = 1, \sigma_u = 0.01$ . For the SPA pole selection  $\mathcal{P}$ , we set the maximum number of closed-loop poles at  $l = 10$ . To form  $\mathcal{P}$  we first incorporate the plant poles and the poles of the desired transfer function. The remaining poles are chosen using two different methods. The first method, which we call the spiral method, involves selecting the remaining poles along an Archimedes spiral as in [6]. The second method, which we call the sparsity-promoting method, involves initially using a spiral which results in an initial collection of 50 poles, and then applying the sparsity-promoting optimization problem from Section IV-B to select the optimal 10 poles for  $\mathcal{P}$  based on the coefficients with the 10 largest Frobenius norms. We also compare the proposed hybrid state space and frequency domain control design method, which we call the hybrid domain method, to the finite time horizon approximation method from [7] with 30 time steps. We solve the SDP for the control design and

the conic program for the sparsity-promoting optimization using MOSEK [11] in conjunction with YALMIP [12] in MATLAB.

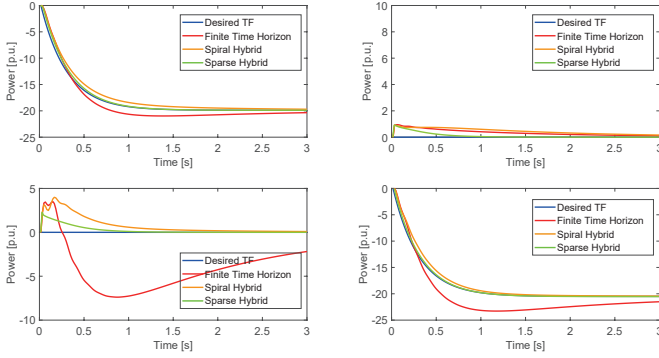


Fig. 1. Step responses of the desired transfer function (Desired TF) and of the solutions of the finite time horizon approximation method with spiral pole selection (Finite Time Horizon), the hybrid domain method with spiral pole selection (Spiral Hybrid), and the hybrid domain method with sparsity-promoting pole selection (Sparse Hybrid).

The step responses for the desired transfer function and the solutions of the finite time horizon approximation method with spiral pole selection [7], the hybrid domain method with spiral pole selection, and the hybrid domain method with sparsity-promoting pole selection are shown in Fig. 1. The proposed hybrid domain method shows much closer matching to the desired step response than the finite time horizon approximation method, even though both methods use the same spiral pole selection, indicating that the absence of truncation error leads to improved performance for our proposed approach. In particular, the finite time horizon approximation method has a much larger deviation and longer transient during the step response. Furthermore, the sparsity-promoting pole selection leads to closer matching to the desired step response than the spiral pole selection, both of which use the hybrid domain method, which suggests that the proposed sparse selection of optimal poles leads to improved performance as well. More specifically, the sparsity-promoting pole selection yields almost perfect matching with the desired response, whereas the spiral selection takes longer to converge to the correct steady state.

## VII. CONCLUSION

In this paper, a novel hybrid state space and frequency domain method for mixed  $\mathcal{H}_2/\mathcal{H}_\infty$  control design was developed. The method uses SLS with SPA, but unlike prior work it does not require any finite time horizon approximations to evaluate the  $\mathcal{H}_2$  and  $\mathcal{H}_\infty$  norms of the closed-loop transfer functions. Therefore, it has reduced suboptimality, improved performance, and less computational cost than prior methods. The state space representations were derived using the KYP lemma applied to a deliberately constructed state space realization in order to obtain a convex and tractable SDP for the control design consisting of LMIs and affine constraints, which can be solved efficiently. To further reduce suboptimality, a sparsity-promoting optimization method was

developed to optimally select a small number of poles from a larger initial collection for use in the control design. This optimization problem was a convex conic program, which again can be efficiently solved. The hybrid domain control design method and the sparsity-promoting optimization were demonstrated on the test case of control design for a wind turbine with power converter interface, and showed superior performance compared to the prior methods. Future work will involve extensions to output feedback and continuous-time control design methods.

## VIII. ACKNOWLEDGEMENT

The second author would like to thank Olle Kjellqvist for the suggestion to consider state space representations for system level synthesis control design. The second author would also like to thank Mingzhou Yin, Andrea Iannelli, and Roy Smith for the recommendation to use atomic norm regularization to enforce sparse pole selection.

## REFERENCES

- [1] D. Youla, H. Jabr, and J. Bongiorno, "Modern wiener-hopf design of optimal controllers—part ii: The multivariable case," *IEEE Transactions on Automatic Control*, vol. 21, no. 3, pp. 319–338, 1976.
- [2] J. Anderson, J. C. Doyle, S. H. Low, and N. Matni, "System level synthesis," *Annual Reviews in Control*, vol. 47, pp. 364–393, 2019.
- [3] L. Furieri, Y. Zheng, A. Papachristodoulou, and M. Kamgarpour, "An input–output parametrization of stabilizing controllers: Amidst youla and system level synthesis," *IEEE Control Systems Letters*, vol. 3, no. 4, pp. 1014–1019, 2019.
- [4] Y. Zheng, L. Furieri, A. Papachristodoulou, N. Li, and M. Kamgarpour, "On the equivalence of youla, system-level, and input–output parameterizations," *IEEE Transactions on Automatic Control*, vol. 66, no. 1, pp. 413–420, 2020.
- [5] Y. Chen and J. Anderson, "System level synthesis with state and input constraints," in *2019 IEEE 58th Conference on Decision and Control (CDC)*, pp. 5258–5263, IEEE, 2019.
- [6] M. W. Fisher, G. Hug, and F. Dörfler, "Approximation by simple poles—part i: Density and geometric convergence rate in hardy space," *IEEE Transactions on Automatic Control*, 2023.
- [7] M. W. Fisher, G. Hug, and F. Dörfler, "Approximation by simple poles—part ii: System level synthesis beyond finite impulse response," *arXiv preprint arXiv:2203.16765*, 2022.
- [8] M. Yin, A. Iannelli, M. Khosravi, A. Parsi, and R. S. Smith, "Linear time-periodic system identification with grouped atomic norm regularization," *IFAC-PapersOnLine*, vol. 53, no. 2, pp. 1237–1242, 2020.
- [9] C. Scherer and S. Weiland, "Linear matrix inequalities in control," *Lecture Notes, Dutch Institute for Systems and Control, Delft, The Netherlands*, vol. 3, no. 2, 2000.
- [10] V. Häberle, M. W. Fisher, E. Prieto-Araujo, and F. Dörfler, "Control design of dynamic virtual power plants: An adaptive divide-and-conquer approach," *IEEE Transactions on Power Systems*, vol. 37, no. 5, pp. 4040–4053, 2021.
- [11] E. D. Andersen and K. D. Andersen, "The mosek interior point optimizer for linear programming: an implementation of the homogeneous algorithm," in *High performance optimization*, pp. 197–232, Springer, 2000.
- [12] J. Lofberg, "Yalmip: A toolbox for modeling and optimization in matlab," in *2004 IEEE international conference on robotics and automation (IEEE Cat. No. 04CH37508)*, pp. 284–289, IEEE, 2004.